

Scientific-Research Article

Static and Dynamic Analyses of Integral Pulse-Width Pulse-Frequency Modulator with Small Error-Reset Integrator Logical Circuit

S. H. Jalali-Naini^{1*}, O. Omid Hemmat²

1-2 Department of Mechanical Engineering, Tarbiat Modares University

ABSTRACT

Keywords: *Integral Pulse-Width Pulse-Frequency Modulator, On-Off Thruster, Spacecraft Attitude, Control*

The static and dynamic analyses of a modified integral pulse-width pulse-frequency (PWPF) modulator with small error-reset integrator (SE-RI) logical circuit are carried out using the grid search method. A set of quasi-normalized equations is utilized to reduce the number of parameters; that is, the integrator gain and the maximum torque of the modulator are merged into other parameters. The output of the modified integral PWPF (IPWPF) modulator is limited to 50 Hertz. The preferred regions of the IPWPF are chosen by the amount of limitation on fuel consumption and thruster firings. These preferred regions are obtained for different dead zone values of the SE-RI circuit. The analyses are performed in two methods with different choices of Schmitt-trigger parameters (i.e., hysteresis or threshold ratio). The proposed regions described by simple inequality equations represent the rectangular regions, which do not give the whole preferred region. As an advantage of the study, the preferred regions are presented graphically instead of rectangular regions by inequality relations.

Nomenclature

A	Sinusoidal input amplitude
DZ	Dead zone of logical circuit
f	Sinusoidal input frequency
H	Hysteresis width
IN	Constant input
k_i	Integrator gain of modulator
N	Number of thruster firings
t_f	Final time
T_{off}	Thruster off-time
T_{on}	Thruster on-time
T_{start}	Duration of the time until modulator turns on
U_{off}	Hysteresis off-threshold
U_{on}	Hysteresis on-threshold

U_m	Maximum torque of modulator
X	Modulator input
Y	Modulator output
ΔV	Fuel consumption

Introduction

Many spacecraft utilize on-off thrusters in their attitude control systems for fast and large angle maneuvers. Since on-off thruster actuators produce discontinuous outputs, it is necessary to modulate the continuous control signals into on-off commands. In this regard, the simplest control algorithm are bang-bang controller with dead zone

1 Assistant Professor (Corresponding Author) **Email:** * shjalalinaini@modares.ac.ir

2 PhD. Candidate

and Schmitt-trigger [1,2]. Several modulators were presented in the past, such as the pulse-frequency modulator, pulse-width pulse-frequency (PWPF) modulator, and the pseudo-rate modulator [3-5]. The integral pulse-width pulse-frequency (IPWPF) modulator is a traditional version of PWPF modulator (PWPFM). This modulator uses an integrator and Schmitt-trigger element in its feed-forward loop and a unity feedback to close the loop [6]. One of this modulator's first practical applications was the on-off attitude control subsystem of the Agena spacecraft [7].

Several methods have been suggested in the literature to tune the parameters of PWPF modulator, including the trial and error method [8], static, dynamic, and system analysis [9-16], the describing function for approximate modeling the Schmitt-trigger element [17] and optimization with meta-heuristic algorithms [18,19]. It is necessary first to obtain allowable/preferred regions of the parameters using static and dynamic analyses. The values obtained from trial and error, optimization and meta-heuristic algorithms must be placed within these allowable/preferred regions of parameters.

The static and dynamic analyses of PWPF modulator were carried out using the grid search method [9-11]. The static and dynamic analyses of pseudo-rate modulator were presented in Refs. [12,13] and compared to those of PWPF modulator. In order to extend the results of the study, the quasi-normalized equations of the static, dynamic, and system analyses in Ref. [14] were utilized to obtain the preferred region of PWPFM parameters using a grid search method [15]. The preferred static and dynamic regions of the parameters in the mentioned analyses were obtained using a grid search method and resulted in the presentation of rectangular-type regions. Subsequently, the quasi-normalized static and dynamic analyses of PWPF modulator in the presence of input noise were performed in Ref. [16], and the preferred regions were obtained with two criteria of fuel consumption and thruster activity.

As mentioned earlier, static analysis of integral PWPF modulator was presented in Ref. [6]. More analysis was carried out in Ref. [20] using quasi-normalized equations and presented Small Error-Reset Integrator (SE-RI) circuit to enhance the performance of the detumbling mode. Moreover, the performance of the modulator in an attitude control loop was compared with that of the PWPF modulator [20].

This paper presents comprehensive static and dynamic analyses of IPWPF modulator with SE-RI circuit using grid search method and approximate equations. Moreover, the uses of normalized fuel consumption and thruster firings are the other advantages over the previous analyses, which provide a more insight to the system behavior. The preferred regions are presented in both graphical and rectangular forms, and it is obvious that rectangular representation may omit some preferred regions.

Static Analysis

In static analysis, the behavior of the modulator is studied outside the attitude control loop by applying a constant input. If the modulator input in the attitude control system is a slowly varying quantity, the static analysis will show a good indication of modulator behavior [11,21,22]. Therefore, the first step in evaluating the attitude control system with the modulator is its static analysis. The static analysis of IPWPF modulator presented in Ref. [6] was led to obtain the relations for modulator off- and on-time, pulse frequency, and modulation factor.

The modified IPWPF modulator with small error-reset integrator (SE-RI) logical circuit is shown in Figure 1 according to Ref. [20]. The SE-RI logical circuit resets the integrator output to zero if the error is small. In Figure 1, X is the input of the modulator, DZ is the value of the integrator reset threshold, U is the input of the Schmitt-trigger and Y is its output, U_{on} is on-threshold, and U_{off} is off-threshold. Also, the difference between the on and off-threshold of the Schmitt-trigger is $H = U_{on} - U_{off}$, which is called the hysteresis width. It should be noted that by using quasi-normalized equations, the output of the Schmitt-trigger is changed to $(0, \pm 1)$, and the integrator's gain is also merged to the on/off-threshold parameter of the Schmitt-trigger. Therefore, the number of parameters of the modulator including DZ is reduced to three.

Since the input is constant, static characteristics of the modified IPWPF modulator for $X > DZ$ are the same as those of the IPWPF modulator. The relations of on-time, off-time, and pulse-width pulse-frequency were obtained in Ref. [6]. Also, the approximate relation for normalized fuel consumption is given by [20]:

$$\frac{\Delta V}{U_m t_f} \approx \frac{T_{on}}{T_{on} + T_{off}} = \frac{IN}{U_m} \quad (1)$$

Equation (1) is obtained by ignoring the value of T_{start} , where T_{start} is the initial on-time. The initial on-

time is a function of $U_{on}/k_i U_m$ and normalized input [20].

The approximate equation for the number of thruster firings (N) is given by

$$N \approx \frac{t_f}{T_{on} + T_{off}} = \frac{\frac{IN}{U_m} (1 - \frac{IN}{U_m})}{\frac{U_{on}}{k_i U_m} - \frac{U_{off}}{k_i U_m}} \quad (2)$$

The maximum value of N is occurred at $X/IN=0.5$, that is,

$$\frac{IN}{U_m} = 0.5 \rightarrow \frac{N_{max}}{t_f} \approx \frac{k_i U_m}{4H} \quad (3)$$

According to Eq. (3), the value of N or N_{max} is inversely proportional to the hysteresis value.

As an example, the modulator's normalized fuel consumption, obtained by numerical solution of quasi-normalized state equations of the system, is depicted in Figure 2 versus $U_{on}/k_i U_m$ and U_{off}/U_{on} for a normalized input of 0.5.

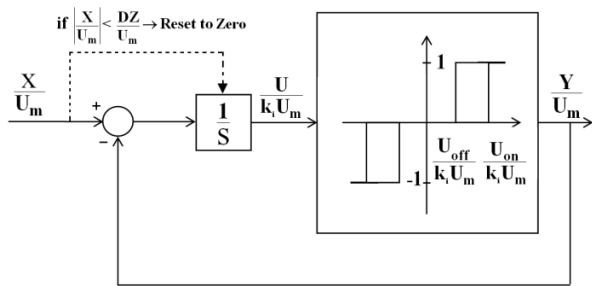


Figure 1. Quasi-normalized block diagram of modified IPWPF modulator

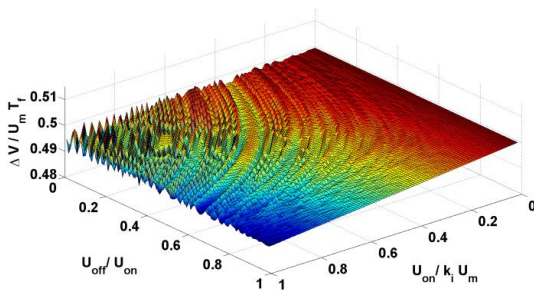


Figure 2. Normalized fuel consumption versus U_{off}/U_{on} and $U_{on}/k_i U_m$ for $X/U_m=0.5$

As shown in Figure 2, normalized fuel consumption, obtained by numerical simulation with final time $t_f = 100$ s is placed within the range of $0.49 < \Delta V/U_m t_f < 0.5$. The value of $\Delta V/U_m t_f = 0.5$ means that the thruster was active for half of the system's operation time. It should be noted that the difference between the results of

Figure 2 and approximate Eq. (1) is due to the ignoring of T_{start} in Eq. (1) that this difference vanishes when $t_f \rightarrow \infty$.

Figure 3 shows the average thruster firings (N/t_f) versus U_{off}/U_{on} and $U_{on}/k_i U_m$ for the normalized input of 0.5 when $U_{on}/k_i U_m > 0.001$. As expected, the value of N increases extremely for the region having both small values of $U_{on}/k_i U_m$ and large values of U_{off}/U_{on} .

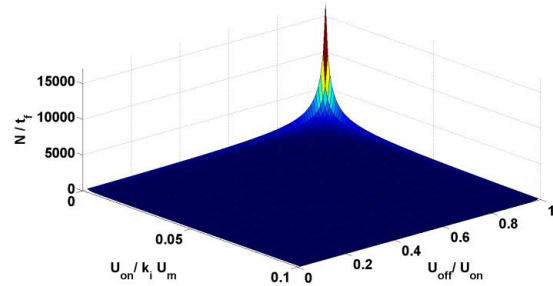


Figure 3. Thruster firings versus U_{off}/U_{on} and $U_{on}/k_i U_m$ for $IN/U_m=0.5$ ($t_f=100$, $U_{on}/k_i U_m > 0.001$)

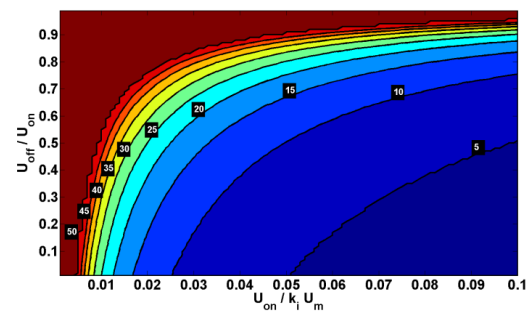
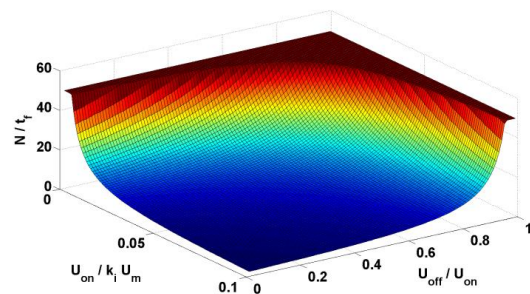


Figure 4. Average thruster firings versus U_{off}/U_{on} and $U_{on}/k_i U_m$ and its contours for $IN/U_m=0.5$ (shown for $N/t_f \leq 50$)

In the figures, the maximum activity of the thruster divided by the final time is limited to 50 (corresponding to the sampling frequency of 100 Hz), whose contours can be seen in two- and three-dimensional representation (see Figure 4). As seen in the figure, the values of N_{max}/t_f larger than 50 are shown by the same color when $N_{max}/t_f = 50$.

The preferred regions of on/off-thresholds can be chosen using Figure 4 based on an allowable thruster firings of $N_{max}/t_f = 5, 10, 15, \dots, 50$.

In order to obtain the preferred regions by assuming the elimination of the upper $\alpha\%$ of the thruster firings, Eq. (2) may be converted into the following equation:

$$\frac{1}{4 \frac{U_{on}}{k_i U_m} (1 - \frac{U_{off}}{U_{on}})} \leq \left(1 - \frac{\alpha}{100}\right) \frac{N_{max}}{t_f} \quad (4)$$

The preferred regions obtained by approximate inequality (4) are agreed with the numerical solution as seen in Figure 5. For example, the contour labeled 10, i.e. allowable average thruster firings=10, is plotted for $\alpha = 80$, that is, the preferred region is chosen by eliminating the upper 80% of $N_{max}/t_f = 50$.

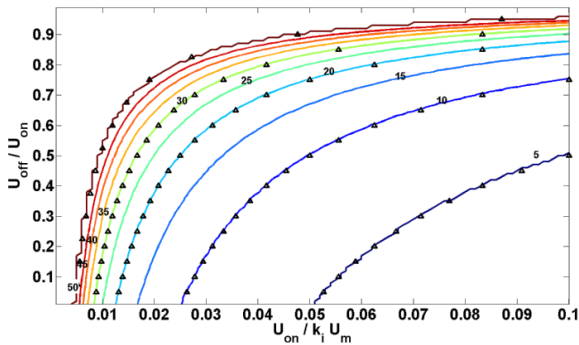


Figure 5. Average thruster firings for different values of $(1-\alpha/100)N_{max}/t_f$: numerical simulation (line) and the approximate inequality (\blacktriangle)

Dynamic Analysis

In dynamic analysis, a sinusoidal signal, $X=A\sin(2\pi ft)$, is usually chosen as the input of the modulator, where A is the amplitude and f is the frequency of the signal. Here, the normalized amplitude, A/U_m , and frequency of the signal vary from 0.25 to 1 and 0.5 to 50 Hz, respectively. In order to obtain the preferred regions of the modulator parameters, two criteria are used: normalized fuel consumption ($\Delta V/U_m t_f$) and total thruster firings divided by final time (N/t_f). The maximum possible normalized fuel consumption is $\Delta V/U_m t_f = 1$, which means the thruster is ON for the entire duration of its operation. On the other hand, the average activity limit of the thruster is assumed to be $N/t_f = 50$, which corresponds to the sampling frequency of 100 Hz. In the following, the preferred regions are obtained based on two combinations of parameters, that is, $U_{on}-U_{off}/U_{on}$ and $H-U_{off}$.

Preferred regions based on $U_{on} - U_{off}/U_{on}$

Here, the preferred regions are obtained by using the two parameters of U_{off}/U_{on} and $U_{on}/k_i U_m$. Figures 6-8 show the normalized representation of fuel consumption for three different values of input frequency $f = 0.5, 5, \text{ and } 50$ Hz.

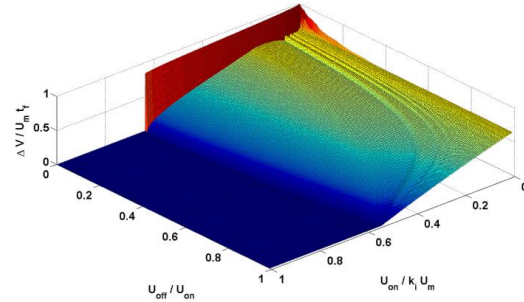


Figure 6. Normalized fuel consumption versus U_{off}/U_{on} and $U_{on}/k_i U_m$ for $A/U_m=1$ and $f = 0.5$ Hz

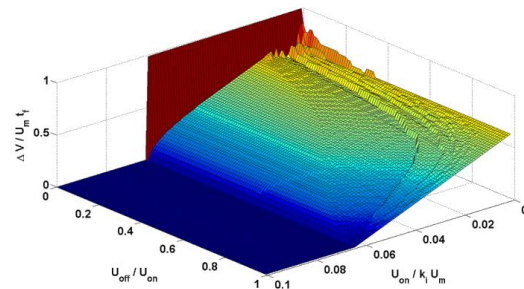


Figure 7. Normalized fuel consumption versus U_{off}/U_{on} and $U_{on}/k_i U_m$ for $A/U_m=1$ and $f = 5$ Hz

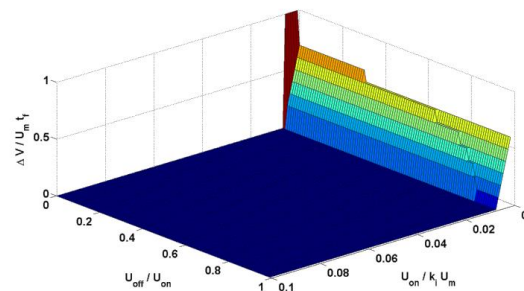


Figure 8. Normalized fuel consumption versus U_{off}/U_{on} and $U_{on}/k_i U_m$ for $A/U_m=1$ and $f = 50$ Hz

As seen in Figures 6-8, by increasing the input frequency, the region of fuel consumption having very small values becomes wider. This behavior can be viewed for the average activity of the thruster, and is depicted in Figures 9-11 for $f = 0.5, 5, \text{ and } 50$ Hz. These figures are plotted for $N/t_f \leq 50$, that is,

the values greater than 50 is shown by the same color when $N/t_f = 50$.

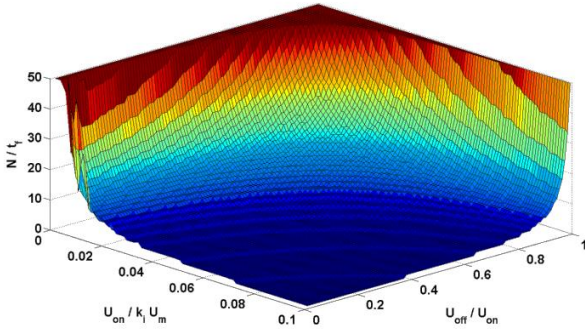


Figure 9. Average thruster firings versus U_{off}/U_{on} and $U_{on}/k_i U_m$ for $A/U_m=1$ and $f = 0.5$ Hz

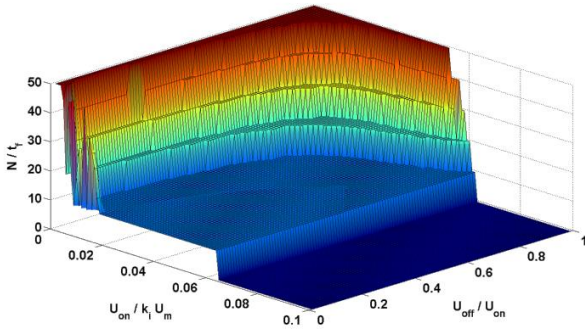


Figure 10. Average thruster firings versus U_{off}/U_{on} and $U_{on}/k_i U_m$ for $A/U_m=1$ and $f = 5$ Hz

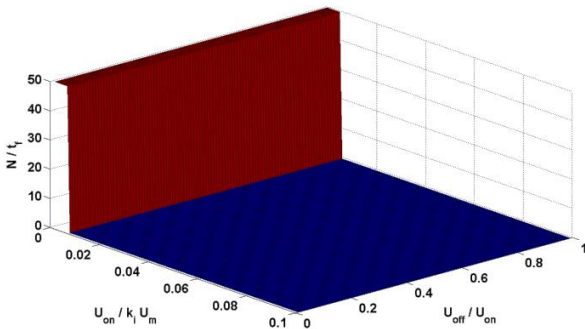
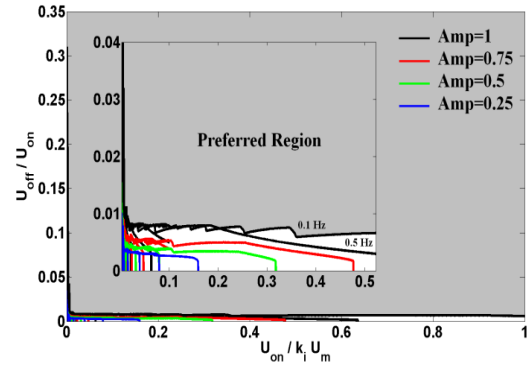


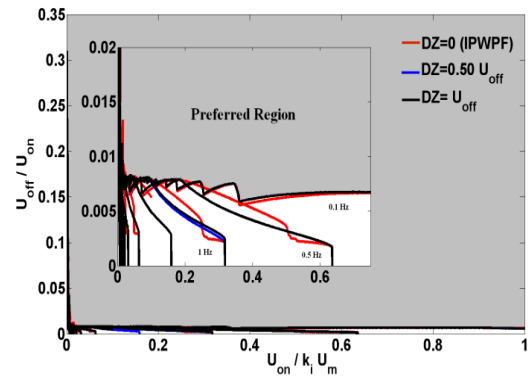
Figure 11. Average thruster firings versus U_{off}/U_{on} and $U_{on}/k_i U_m$ for $A/U_m=1$ and $f = 50$ Hz

Here, the preferred regions of the modulator parameters are chosen by eliminating the upper 30% of the normalized fuel consumption ($\Delta V/U_{m t_f} \leq 0.7$). Figure 12 shows the contours of $\Delta V/U_{m t_f} = 0.7$ for frequencies of 0.1 to 50 Hz and $A/U_m = 0.25, 0.5, 0.75, 1$ for three different values of dead zones DZ

= 0, $0.5U_{off}$, U_{off} . The preferred region of the modulator parameters is distinguished in gray color.



a) $A/U_m = 0.25, 0.5, 0.75, 1$ and $DZ = U_{off}$



b) $DZ = 0, 0.5U_{off}, U_{off}$ and $A/U_m = 1$

Figure 12. Preferred region based on $\Delta V/U_{m t_f} \leq 0.7$ for the input range of frequencies $f = 0.1$ to 50 Hz

The fuel consumption contours show that the lower bound of the preferred region is $U_{off}/U_{on} > 0.009$ when $U_{on}/k_i U_m$ is chosen > 0.016 , or the preferred region is given by $U_{off}/U_{on} > 0.31$ for $U_{on}/k_i U_m > 0.001$ ($A/U_m = 0.25, 0.5, 0.75, 1$). This is the disadvantage of preferred regions in rectangular-type representation. This type of representation omits some preferred regions. It is worth noting that by eliminating the upper 50% of fuel consumption ($\Delta V/U_{m t_f} \leq 0.5$), the obtained regions are not applicable/reasonable, and therefore, the graphs are not provided. According to Figure 12, the presence of dead zone, by assuming the elimination of the upper 30% of fuel consumption, has a negligible effect on the preferred regions, and the above-mentioned preferred regions can be chosen for IPWPF modulators with/without SE-RI circuit, based on fuel consumption criterion.

In the following, the preferred regions are chosen by assuming the elimination of the upper 30% (and

50%) of the maximum allowable average thruster firings (here given by 50 times per second). Figure 13 shows the preferred regions, distinguished by gray color, corresponding to $N/t_f < 25, 35$ for sinusoidal input amplitude of $A/U_m = 0.25, 0.5, 0.75, 1$ and input frequency of $f = 0.1$ to 50 Hz. Based on the analysis of the thruster firings criterion in Figure 13, the preferred regions show slight differences between the two studied cases. In our thruster firings analysis, the important point is that the preferred region cannot be obtained only by a unit sinusoidal input. For instance, the bound of preferred region is constructed by $A/U_m = 1$ only for $0.005 < U_{off}/U_{on} < 0.64$ in Case a, whereas this bound is constructed by $A/U_m = 0.5 \sim 0.75$ for $U_{off}/U_{on} > 0.64$, as seen in Figure 13.

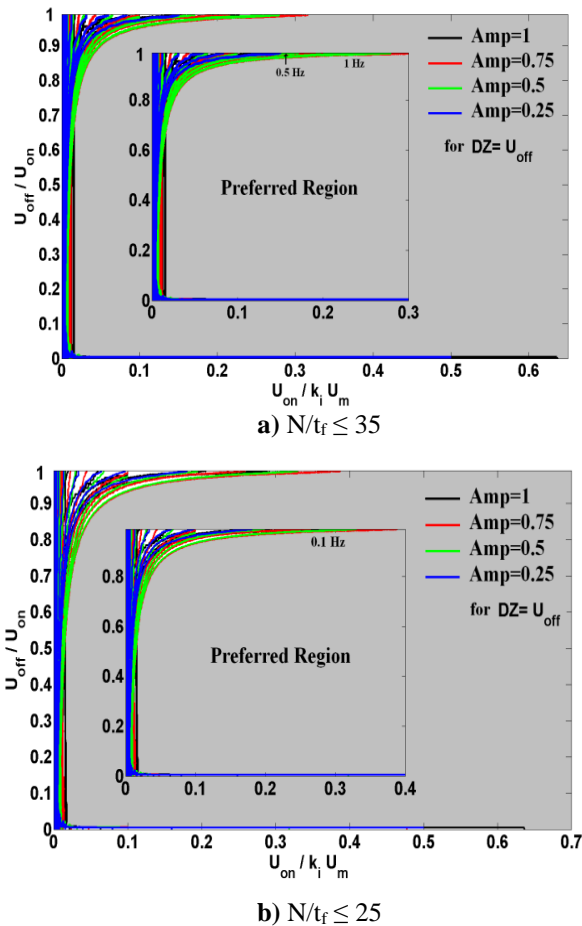


Figure 13. Preferred region based on a) $N/t_f \leq 35$ and b) $N/t_f \leq 25$ for the range of frequencies $f = 0.1$ to 50 Hz ($A/U_m = 0.25, 0.5, 0.75, 1$)

Preferred regions based on H - U_{off}

In the second representation of figures in our analysis, the preferred regions are extracted based on the two parameters of $U_{off}/k_i U_m$ and $H/k_i U_m$. The normalized fuel consumption versus $U_{off}/k_i U_m$ and

$H/k_i U_m$ are depicted in Figures 15-17 for $A/U_m = 1$ and $f = 0.5, 5, 50$. It is evident that by increasing the sinusoidal input frequency, the range in which the fuel consumption has smaller values becomes wider. This is also true about the average thruster firings (N/t_f). Figures 18-20 show the average thruster firings (N/t_f) versus $U_{off}/k_i U_m$ and $H/k_i U_m$ for $A/U_m = 1$ and $f = 0.5, 5, 50$ in quasi-normalized form.

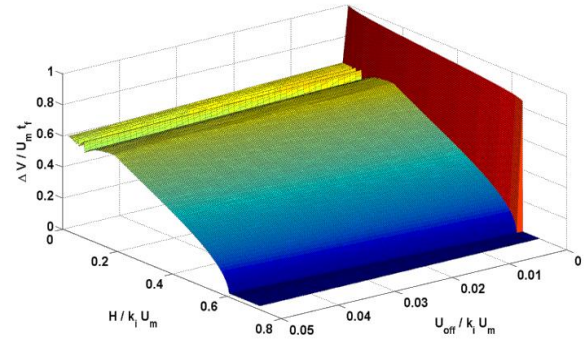


Figure 15. Fuel consumption versus H and U_{off} in normalized form for $A/U_m = 1$ and $f = 0.5$ Hz

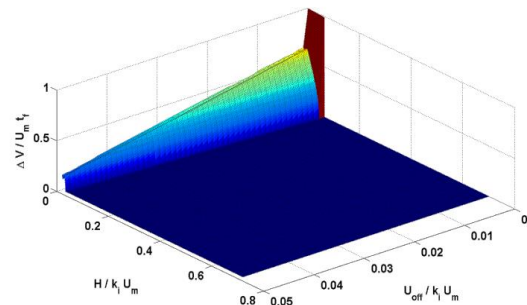


Figure 16. Fuel consumption versus H and U_{off} in normalized form for $A/U_m = 1$ and $f = 5$ Hz

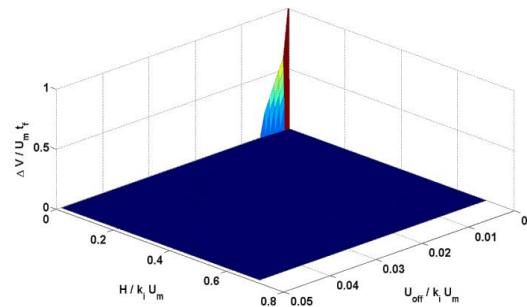


Figure 17. Fuel consumption versus H and U_{off} in normalized form for $A/U_m = 1$ and $f = 50$ Hz

The preferred regions for the criteria of $\Delta V/U_m t_f \leq 0.7$ and $N/t_f \leq 35$ are depicted in Figures 21 and 22 based on H- U_{off} graph, respectively, when the sinusoidal input frequency varies from a minimum value of 0.1 or 5 Hz to 50 Hz ($A/U_m = 0.25, 0.5, 0.75, 1$ and $DZ = 0, U_{off}$). The preferred region of the modulator parameters in each figure is distinguished

in gray color. As seen in Figure 21, if $U_{off}/k_i U_m$ is chosen greater than 0.00082, the normalized fuel consumption remains less than 0.7, regardless of the value of normalized hysteresis width.

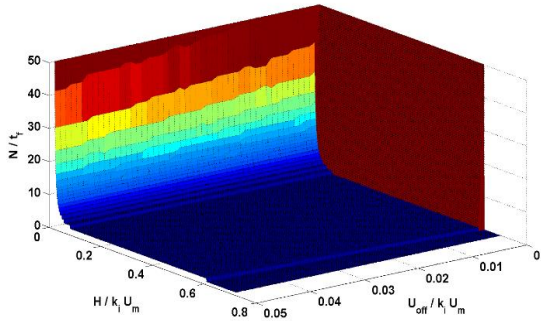


Figure 18. Average thruster firings versus H and U_{off} in quasi-normalized form for $A/U_m=1$ and $f = 0.5$ Hz

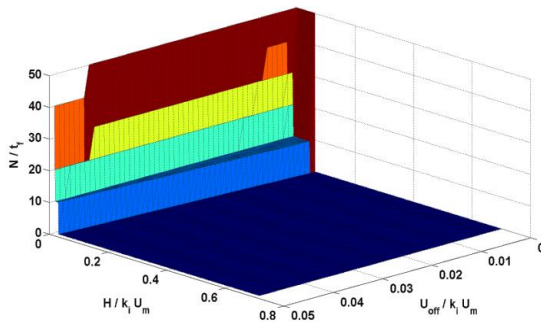


Figure 19. Average thruster firings versus H and U_{off} in quasi-normalized form for $A/U_m=1$ and $f = 5$ Hz

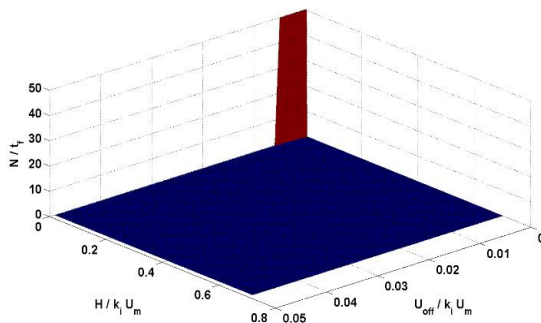


Figure 20. Average thruster firings versus H and U_{off} in quasi-normalized form for $A/U_m=1$ and $f = 50$ Hz

Our analysis based on Figures 23 and 24 shows that the preferred regions, obtained by a unit sinusoidal input, cover the regions that are related to the sinusoidal inputs with lower amplitudes as the worst case (note that $A/U_m = 0.25, 0.5, 0.75$ and 1 are only checked). In other words, the boundary of the preferred region is obtained by unit sinusoidal input by eliminating the upper 30% of fuel consumption (or average thruster firings). The changes of the preferred region due to different values for $0 \leq DZ$

$\leq U_{off}$ are negligible, and the figures are not provided.

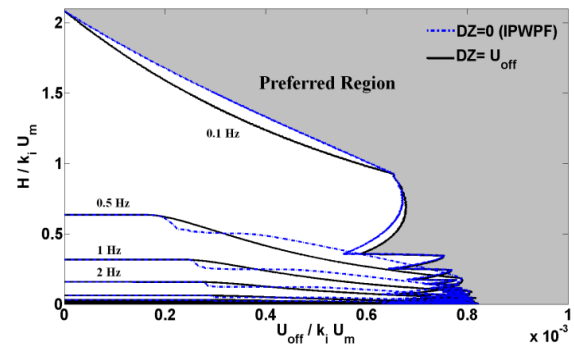


Figure 21. Preferred regions for $\Delta V/U_{mtr} \leq 0.7$ for different minimum values of the range of frequencies

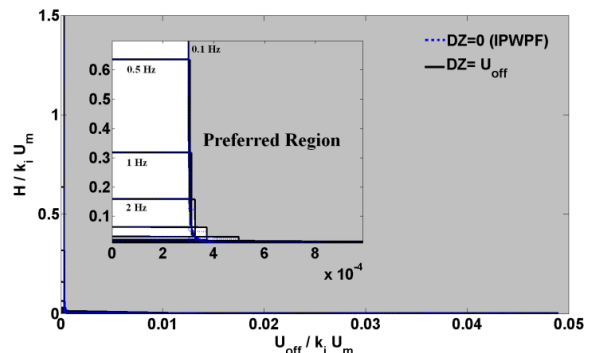


Figure 22. Preferred regions for $N/t_f \leq 35$ for different minimum values of the range of frequencies

Figure 25 shows the preferred regions for $N/t_f \leq 25$ based on $H-U_{off}$ graph when the input frequency varies from 0.1 to 50 Hz ($A/U_m=1, DZ=0, U_{off}$). The preferred region of the modulator parameters is distinguished in gray color. The dynamic analysis has also been carried out by elimination of the upper 50% of the average thruster firings. For this case, the analysis suffices only for a unit sinusoidal input within the range of $0 \leq U_{off}/k_i U_m \leq 0.05$ as in our analysis for the upper 70% of the average thruster firings. As mention earlier, the preferred regions for $\Delta V/U_{mtr} \leq 0.5$ are not applicable and the figures are not provided.

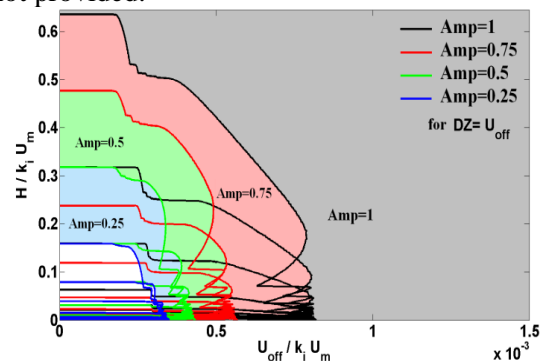


Figure 23. Preferred regions for $\Delta V/U_{mtr} \leq 0.7$ for the range of frequencies $f = 0.1$ to 50 Hz ($A/U_m = 0.25, 0.5, 0.75, 1$)

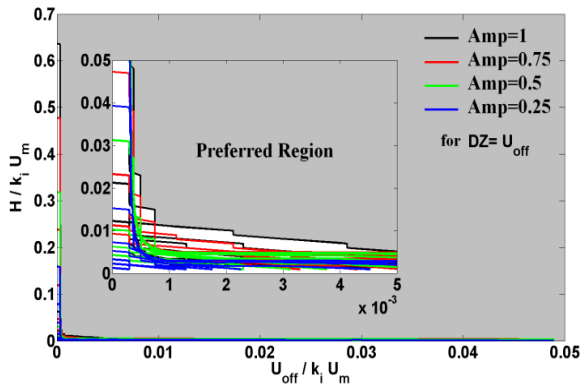


Figure 24. Preferred regions for $N/t_f \leq 35$ for the range of frequencies $f = 0.1$ to 50 Hz ($A/U_m = 0.25, 0.5, 0.75, 1$)

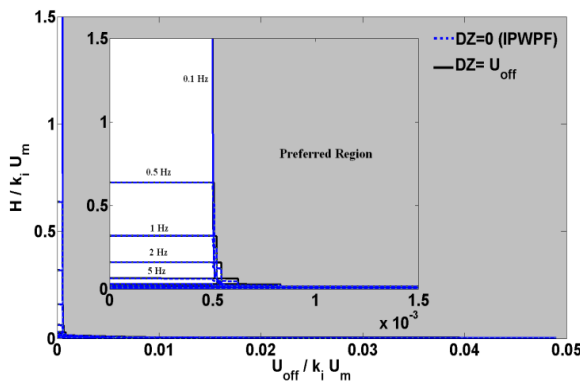


Figure 25. Preferred regions for $N/t_f \leq 25$ for the range of frequencies $f = 0.1$ to 50 Hz ($DZ = 0, U_{off}$)

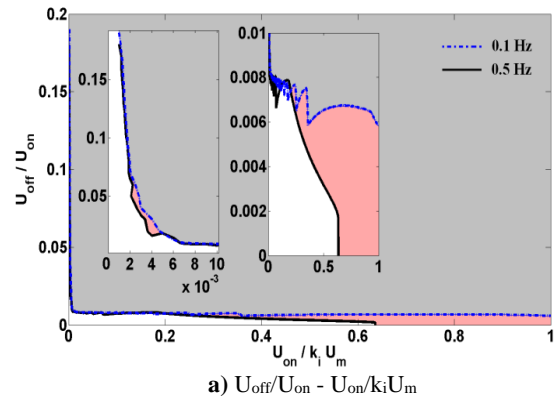
Discussion

Dynamic analysis of modified integral PWPF modulator with dead zone has been performed by two combinations of parameters, that is, $H-U_{off}$ and $U_{off}-U_{off}/U_{on}$. The normalized amplitude, A/U_m , and frequency of the sinusoidal input vary from 0.25 to 1 and 0.5 to 50 Hz, respectively.

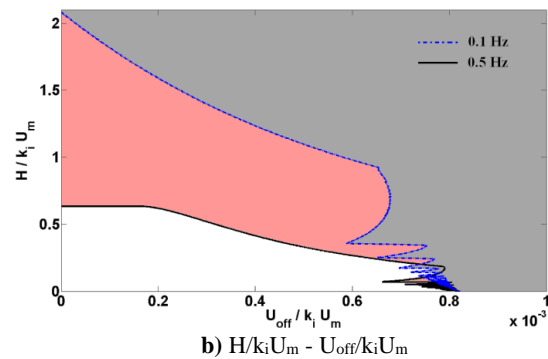
In most literature, the preferred regions for PWPF modulator have led to rectangular regions which do not include some allowable regions. Here, the preferred regions have also been presented as a first step in the form of rectangular regions for IPWPF modulator. In order to determine the preferred region, an appropriate graphical representation has been chosen. Our graphical representation gives all preferred regions that satisfy the performance criterion on the contrary of rectangular-type representation. The results of our study are summarized in Figures 26 and 27.

To select the appropriate parameters of IPWPF based on the elimination of the upper 30% of fuel consumption, the preferred region and its boundary are shown in Figure 26. As seen in the figure, this graph is obtained for two ranges of frequencies, $f =$

0.1 to 50 Hz and $f = 0.5$ to 50 Hz. Although the frequency of 0.1 Hz is not reasonable for dynamic analysis, the graph is only provided for comparison with the boundary of preferred region produced by a minimum frequency of 0.5 Hz. As a rectangular-type description of preferred region, the inequality of $U_{off}/k_i U_m > 0.00082$ satisfy the fuel consumption criterion for the frequency range of $f=0.1$ to 50 Hz.

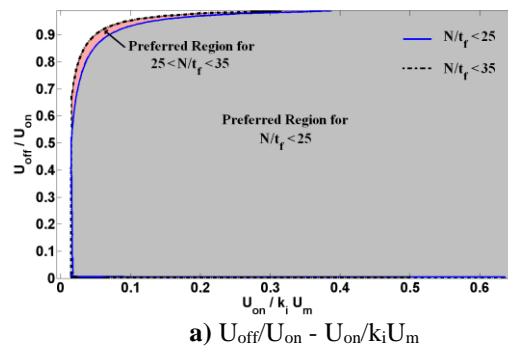


a) $U_{off}/U_{on} - U_{on}/k_i U_m$



b) $H/k_i U_m - U_{off}/k_i U_m$

Figure 26. Preferred region of IPWPF for $f = 0.1-50$ Hz and $f = 0.5-50$ Hz based on $\Delta V/U_m t_f \leq 0.7$ in two combinations of parameters ($DZ = U_{off}$)



a) $U_{off}/U_{on} - U_{on}/k_i U_m$

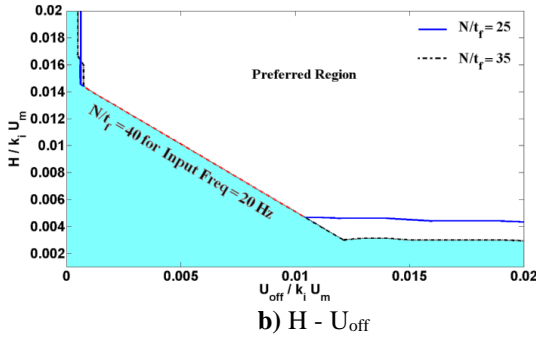


Figure 27. Preferred regions of the average thruster firings for $N/t_f \leq 25, 35$ ($DZ = U_{off}$)

The preferred region of the IPWPF parameters is given in Figure 27 based on two different values of thruster firings limits $N/t_f \leq 25, 35$. It is worth noting that at the location of the red dashed-line in Figure 27b, the average thruster firings jumps about 40 units for the input frequency of 20 Hz.

Approximate Eq. (1) implies that the amount of normalized fuel consumption is equal to the normalized input (I_N/U_m) for static analysis when $I_N > DZ$, regardless of the other parameters values. The preferred regions for different values of the thruster firings limit $N/t_f = 5, 15, 25, \text{ and } 35$ are also seen in Table 1.

Table 1. Preferred regions in the static analysis of modified IPWPF according to Eq. (4)

Preferred region ($H/k_i U_m > 0.001$)	Criterion
$H/k_i U_m > 0.007$	$N/t_f < 35$
$H/k_i U_m > 0.01$	$N/t_f < 25$
$H/k_i U_m > 0.017$	$N/t_f < 15$
$H/k_i U_m > 0.05$	$N/t_f < 5$

The preferred regions have been observed using dynamic analysis by plotting the relevant contours in Figures 26 and 27. From these figures, we are now to extract a rectangular region within preferred region for the input frequencies of 0.5 to 50 Hz in our dynamic analysis as viewed in Table 2. It is worth noting that the nature of displaying of regions in a rectangular form is that it is possible to suggest different rectangles. For example, two choices of rectangular-type regions are seen in the third column of the first row of Table 2 that each of them omits some parts of the whole preferred region. On the other hand, the regions provided in the second

column of the table, specify the equivalent rectangular regions according to the two choices of combinations of parameters, that is, $H-U_{off}$ and $U_{on}-U_{off}/U_{on}$.

Table 2. Preferred regions in dynamic analysis of modified IPWPF ($DZ = U_{off}$)

Criterion	Dynamic analysis $H-U_{off}$	Dynamic analysis $U_{on}-U_{off}/U_{on}$
$\Delta V/U_{mt} \leq 0.7$	$H/k_i U_m > 0.001$ for $U_{off}/k_i U_m > 0.00082$ or $H/k_i U_m > 0.001$ for $U_{on}/k_i U_m > 0.0018$ Figure 26b	First choice: $U_{off}/U_{on} > 0.009$ for $U_{on}/k_i U_m > 0.007$ Second choice: $U_{off}/U_{on} > 0.18$ for $U_{on}/k_i U_m > 0.001$ Figure 26a
$N/t_f \leq 35$	$H/k_i U_m > 0.0144$ for $U_{off}/k_i U_m > 0.0007$ or $H/k_i U_m > 0.0144$ for $U_{on}/k_i U_m > 0.0151$ Figure 27b	$0.0138 < U_{off}/U_{on} < 0.68$ & $U_{on}/k_i U_m > 0.015$ Figure 27a
$N/t_f \leq 25$	$H/k_i U_m > 0.0146$ for $U_{off}/k_i U_m > 0.0006$ or $H/k_i U_m > 0.0166$ for $U_{on}/k_i U_m > 0.0152$ Figure 27b	$0.02 < U_{off}/U_{on} < 0.57$ & $U_{on}/k_i U_m > 0.01$ Figure 27a

Conclusions

The static and dynamic analyses of a modified integral pulse-width pulse-frequency (PWPF) modulator with small error-reset integrator (SE-RI) logical circuit are carried out using the grid search method. A set of quasi-normalized equations is utilized to reduce the number of parameters; that is, the integrator gain and the maximum torque of the modulator are merged into other parameters. The average thruster activity of the modified integral PWPF (IPWPF) modulator is limited to 50 Hz. The preferred regions of the IPWPF are chosen by the amount of limitation on fuel consumption and thruster firings.

In this study, the static and dynamic analyses of a modified integral pulse-width pulse-frequency modulator (IPWPF) are performed using quasi-normalized equations. The modified IPWPF benefits a SE-RI logical circuit. The analyses are carried out for three different values of the dead zone of SE-RI circuit ($DZ = 0, 0.5U_{off}, U_{off}$). In the static analysis, the preferred regions are obtained using approximate relation, verified by numerical solution for different values of allowable average thruster firings.

The dynamic analysis is done for the range of input frequencies between 0.5 and 50 Hz for the normalized input amplitude = 0.25, 0.5, 0.75, 1 and dead zone = 0, $0.5U_{off}$, U_{off} . The results show that the dynamic analysis using unit amplitude suffices for fuel consumption criterion whereas for thruster activity analysis it is necessary to consider the amplitudes less than 1. In addition, using the appropriate method of displaying the all contours in the graphs, the boundary of the preferred region is obtained by changing the input amplitude and frequency together. This type of representation gives a wider preferred region than rectangular type. Moreover, the preferred regions are obtained by eliminating the upper 30% and 50% of the two performance criteria of fuel consumption and the average thruster firings (with the limit of 50 Hz). The mentioned analysis is performed with two sets of parameters $U_{off}/U_{on}-U_{on}$ and $H-U_{off}$. Finally, the rectangular regions that include only a part of the preferred regions are also presented.

References

- [1] Bryson, A. E., *Control of Spacecraft and Aircraft*, 1st Ed., Princeton University Press, 1994.
- [2] Brown, C. D., *Elements of Spacecraft Design*, AIAA, Reston, Virginia, 2002.
- [3] Werts, R., *Spacecraft Attitude Determination and Control*, Kluwer Academic Publisher, 1978.
- [4] Sidi, M. J., *Spacecraft Dynamic and Control*, Cambridge University Press, 1997.
- [5] Mathavaraj, S. and Padhi, R., *Satellite Orbital Dynamics*, Springer, 2021.
- [6] Feron, E., "Pulse Modulation," Lecture Note, MIT University.
- [7] Kunkle, J. L., "The Agena Pneumatic System-Control Gas Requirements Stability and Response," *LXSC/A313082*, Lockheed Missiles and Space Corporation, Sunnyvale, Calif.
- [8] Rouzegar, H., Khosravi, A. and Sarhadi, P., "Vibration Suppression and Attitude Control for the Formation Flight of Flexible Satellites by Optimally Tuned On-Off State-Dependent Riccati Equation Approach," *Transactions of the Institute of Measurement and Control*, Vol. 42, No. 15, 2020, pp. 2984-3001.
- [9] Wie, B., *Space Vehicle Dynamics and Control*, AIAA Education Series, Reston, Virginia, 1998.
- [10] Song, G. and Buck, N., "Spacecraft Vibration Reduction Using Pulse-Width Pulse-Frequency Modulated Input Shaper," *Journal of Guidance, control, and Dynamics*, Vol. 22, No. 3, 1999, pp. 433-440.
- [11] Krovel, T. D., *Optimal Tuning of PWPF Modulator for Attitude Control*, MS Thesis, Norwegian University of Science and Technology, Trondheim, 2005.
- [12] Navabi, M. and Rangraz, H., "Comparing Optimum Operation of Pulse Width-Pulse Frequency and Pseudo-Rate Modulators in Spacecraft Attitude Control Subsystem Employing Thruster," *Recent Advances in Space Technologies (RAST)*, 2013, pp. 625-630.
- [13] Navabi, M. and Rangraz, H., "Comparing Optimum Operation of Pulse Width-Pulse Frequency and Pseudo-Rate Modulators Regarding Subsystem Life Duration in Control Subsystem Employing Thruster," *The 12th Conference of Iranian Aerospace Society*, 2013.
- [14] Jalali-Naini, S. H., "Static Analysis of Pulse-Width Pulse-Frequency Modulator Based on Analytical and Numerical Solutions," *Journal of Space Science and Technology*, Vol. 11, No. 1, pp. 13-29, 2018 (in Persian).
- [15] Jalali-Naini, S. H. and Ahmadi Darani, S., "Preliminary Design of Spacecraft Attitude Control with Pulse-Width Pulse-Frequency Modulator for Rest-to-Rest Maneuvers," *JAST*, Vol. 11, No. 1, pp. 1-8, 2017.
- [16] Jalali-Naini, S. H. and Bohlouri, V., "Quasi-Normalized Static and Dynamic Analysis of Pulse-Width Pulse-Frequency Modulator in Presence of Input Noise," *Modares Mechanical Engineering*, Vol. 16, No. 2, pp. 455-466, 2017.
- [17] Mazinan, A. H., "On Pulse-Width Pulse-Frequency Modulator Control Strategy: An Adaptation-Based Describing Function Representation," *Sāzhanā*, Vol. 45, No. 1, 2020, pp. 1-5.
- [18] Khosravi, A. and Sarhadi, P., "Tuning of Pulse-Width Pulse-Frequency Modulator Using PSO: An Engineering Approach to Spacecraft Attitude Controller Design," *Automatika*, Vol. 57, No. 1, 2016, pp. 212-220.
- [19] Khalili, N. and Ghorbanpour, A., "Optimal Tuning of Single-Axis Satellite Attitude Control Parameters Using Genetic Algorithm," *In Dynamic Systems and Control Conference*, Vol. 84287, p. V002T36A003. *American Society of Mechanical Engineers*, 2020.
- [20] Jalali-Naini, S. H. and Omid Hemmat, O., "A Modification to Integral Pulse-Width Pulse-Frequency Modulator," *Journal of Space Science and Technology*, Vol. 14, No. 1, pp. 55-64, 2021 (in Persian).
- [21] Anthony, T. C. and Wie, B., "Pulse-Modulated Control Synthesis for a Flexible Spacecraft," *Journal of Guidance, Control, and Dynamics*, Vol. 13, No. 6, 1990, pp. 1014-1022.
- [22] Soumya, N. and Nair, P., "Attitude Control Schemes for Crew Module Atmospheric Re-entry Experiment Mission," *IFAC*, Vol. 51, No. 1, 2018, pp. 627-632.

COPYRIGHTS

©2022 by the authors. Published by Iranian Aerospace Society This article is an open access article distributed under the terms and conditions of the Creative Commons Attribution 4.0 International (CC BY 4.0) <https://creativecommons.org/licenses/by/4.0/>

